

# Six-phase doubly fed induction machine-based standalone DC voltage generator

Paweł MACIEJEWSKI and Grzegorz IWAŃSKI\*

Warsaw University of Technology, Institute of Control and Industrial Electronics, 75, Koszykowa St., 00-662 Warszawa, Poland

**Abstract.** The paper presents a multi-phase doubly fed induction machine operating as a DC voltage generator. The machine consists of a six-phase stator circuit and a three-phase rotor circuit. Two three-phase six-pulse diode rectifiers are connected to each three-phase machine section on the stator side and in parallel to the common DC circuit feeding the isolated load. The same DC bus is also common for the rotor side power electronics converter responsible for machine control. Two methods – direct torque control DTC and field oriented control FOC – were implemented for machine control and compared by means of simulation tests. Field oriented control was implemented in the laboratory test bench.

**Key words:** six-phase induction machine; induction generator; torque oscillations; DC voltage generation.

## 1. Introduction

The classic three-phase doubly fed induction generator (DFIG) is one of the most popular types of machines used for wind turbines. Recent standards in the field of grid connection of power sources are becoming more and more restrictive and in some cases, such as grid voltage dips (especially asymmetrical ones), they cannot be met by DFIG, because at these transient states high voltage is induced on the rotor side. The problem is a minor issue in a doubly fed induction generator of DC voltage (DFIG-DC) recently proposed by *Marques and Iacchetti* [1–3] and later studied extensively by several teams.

A six-pulse diode rectifier connected to the stator side of an induction machine not only introduces stator current harmonics, but it also deforms stator voltage as well as stator flux waveforms [4] and, consequently, introduces electromagnetic torque pulsations. In the studied DFIG-DC system, a typical field oriented control method does not reduce torque ripples significantly in relation to open loop control. This is because torque is not controlled directly, but current vector components are. Introduction of an additional transformer between stator and diode rectifier for improving the stator current and stator flux waveforms [5] is not a reasonable method for machine torque ripples reduction.

An active filter has been used in [6] for reduction of harmonics, but this approach requires an additional converter (active filter), the rated current of which is not much smaller than the total power flowing through the diode rectifier. Mitigation of the torque ripples problem by means of various control methods of the rotor converter (RC) instead of applying

additional converters acting as harmonics filters is therefore studied.

To reduce torque pulsations in a three-phase DFIG-DC system, resonant controllers of electromagnetic torque [7, 8] are usually proposed, forcing adequate harmonics of the current vector component or rotor voltage vector component in control paths responsible for torque control. As the control algorithms with resonant terms are sensitive to frequency changes, on-line tuning of the resonant frequency of these terms is required. Repetitive algorithm based control for torque ripples reduction can be also applied [9] as a parallel control path to the main torque control loop.

Direct torque control with hysteresis controllers was evaluated for a DFIG-DC generating system in [10]. As hysteresis controllers based DTC is fast, low frequency torque oscillations can be significantly reduced in relation to field oriented control, but switching harmonics content in the current causes larger torque high frequency ripples at the same average switching frequency. The switching frequency ripples in the DTC method can be reduced by the use of a PWM modulator and linear controllers [11, 12].

Reduction of harmonics, i.e. torque pulsation, can be achieved by increasing the number of voltage pulses. For the classic three-phase generator, this approach requires a dedicated transformer multiplying the number of voltage pulses, which increases the cost of the system. In recent years, multi-phase electrical power generators have been increasingly attracting the attention of researchers [13–15]. This type of electrical machines can achieve significant torque pulsation reduction of certain torque harmonics, depending on the winding configuration [16]. Moreover, additional phases render post-fault operation possible along with reduction of stator copper losses in comparison to 3-phase machines [17, 18].

Studies on multi-phase machines focus mainly on permanent magnet synchronous machines, brushless DC machines,

\*e-mail: iwanskig@isep.pw.edu.pl

Manuscript submitted 2020-06-04, revised 2020-09-25, initially accepted for publication 2020-10-15, published in February 2021

cage induction machines and switched reluctance machines, but the doubly fed induction machine has not been a topic of interest due to its main application in grid connected systems.

In [19], the three-phase stator and six-phase rotor doubly fed induction machine has been shown with the grid connected stator and the rotor circuit divided into two three-phase sections. This solution increases the number of slip rings – brushes sets. It has to be noted that for generation operation the speed range is limited and the power of the electronic converter is nonetheless fractional in relation to the total power, and the three phases of a rotor circuit may be retained so as not to increase the number of slip-rings and brushes.

Although the rotor side of the machine transfers fractional power, the stator side of the machine transfers a major part of the energy generated to the DC bus through a diode rectifier producing stator current harmonics influencing torque ripples. That is why an increase in the number of stator phases can be of interest, taking account of the potential reduction of torque oscillations. The model of the three-phase rotor and six-phase stator doubly fed induction machine for a DFIG-DC system has already been shown in [20], with open loop control and simulation results only. Some discussion on twelve-pulse rectification and rotor current harmonics reduction and electromagnetic torque oscillations reduction using six-phase stator machine is provided in [21], based on simulation results as well. The three-phase rotor and six-phase stator doubly fed induction machine was reported also for an AC generating system in [22].

In this paper, a DFIG-DC generator with the new multi-phase doubly fed induction machine with a twelve-pulse diode rectifier is shown, followed by experimental validation. Twelve pulses are achieved by shifting three-phase sections of the machine by 30 degrees. The scheme of the proposed DFIG-DC system with a six-phase stator and two six-pulse diode rectifiers (DR1, DR2) is shown in Fig. 1. The marked direction of stator current flow is in accordance with the standard model of the induction machine.

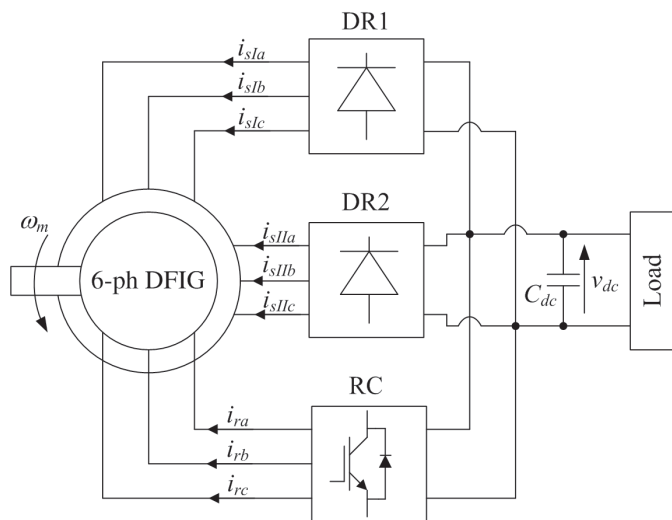


Fig. 1. Scheme of the DFIG-DC voltage generator with a six-phase stator and three-phase rotor doubly fed induction machine

## 2. System description and modeling

Multi-phase machines can be divided into two main groups – those with symmetrical and asymmetrical stator phases distribution. In symmetrical machines, all stator phases are shifted by the same angle, whereas asymmetrical machines have a different shift angle between phases. Winding sections can have a common neutral point or they may have separate neutral points, as shown in Fig. 2. In literature, a six-phase machine with separate three-phase sections is called a double three-phase machine [23]. In the case of a multi-phase DFIG, the machine rotor can be three-phase, just like in a classic three-phase machine, in order to reduce the number of slip-rings.

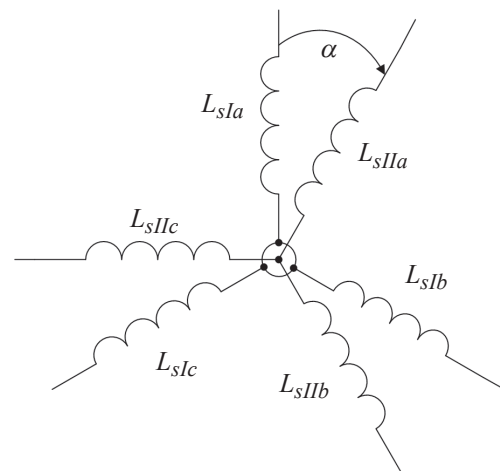


Fig. 2. Scheme of stator windings connection of a six-phase DFIG

The six-phase cage induction machine with asymmetrical distribution of stator windings sections was thoroughly analyzed for operation with thyristor converters due to the natural property of the machine, which is a lack of the influence of stator voltage (thus flux) harmonics  $6k \pm 1$  ( $k = 1, 3, 5 \dots$ ) on electromagnetic torque [24]. This results in cancelation of 6<sup>th</sup> harmonic as well as its odd multiples in torque oscillations, caused by the nonlinear rectifier.

In the model, the following assumptions are made:

- the flux path is linear,
- the windings parameters are identical,
- there is sinusoidal distribution of magnetic induction,
- inductance is not a function of the shift angle.

Voltage equations of a doubly fed induction machine in a stationary frame are as follows (1, 2):

$$\mathbf{v}_s = \mathbf{R}_s \mathbf{i}_s + \frac{d}{dt} \Psi_s, \quad (1)$$

$$\mathbf{v}_r = \mathbf{R}_r \mathbf{i}_r + \frac{d}{dt} \Psi_r - jp\omega_m \Psi_r. \quad (2)$$

Flux equations are described by (3, 4):

$$\Psi_s = \mathbf{M}_{rs} \mathbf{i}_r + \mathbf{L}_s \mathbf{i}_s, \quad (3)$$

## Six-phase doubly fed induction machine-based standalone DC voltage generator

$$\Psi_r = M_{sr}i_s + L_r i_r. \quad (4)$$

Electromagnetic torque can be derived from magnetic coenergy Eq. (5):

$$T_e = p i_s^T \left( \frac{d}{d\theta} M_{sr} \right) i_r. \quad (5)$$

Matrices  $R_s$ ,  $R_r$ ,  $L_s$ ,  $L_r$ ,  $M_{rs}$ ,  $M_{sr}$ ,  $\frac{d}{d\theta} M_{sr}$  are all included in the appendix, and  $p$  is the number of pole pairs.

Park's transformation is a mathematical tool, fundamental for vector control. It results in decomposition of a three-phase system to a vector with components  $dq$ . In the case of asymmetrical multiphase machines, a 6-phase Park's transformation  $T_{6f}$  (in the appendix) is applied, resulting in additional non-electromotive force producing components. Stator voltage equation (1) in a stationary frame can be transformed to the rotating frame (6).

$$T_{6f} v_s = T_{6f} R_s i_s + T_{6f} \frac{d}{dt} \Psi_s, \quad (6)$$

and following decomposition to  $dq$ ,  $xy$  and  $0_1 0_2$ , components Eqs (7–12) can be obtained:

$$v_{sd} = R_s i_{sd} + \frac{d}{dt} \Psi_{sd} - \omega_s \Psi_{sd}, \quad (7)$$

$$v_{sq} = R_s i_{sq} + \frac{d}{dt} \Psi_{sq} - \omega_s \Psi_{sq}, \quad (8)$$

$$v_{sx} = R_s i_{sx} + \frac{d}{dt} \Psi_{sx}, \quad (9)$$

$$v_{sy} = R_s i_{sy} + \frac{d}{dt} \Psi_{sy}, \quad (10)$$

$$v_{s01} = R_s i_{s01} + \frac{d}{dt} \Psi_{s01}, \quad (11)$$

$$v_{s02} = R_s i_{s02} + \frac{d}{dt} \Psi_{s02}. \quad (12)$$

Similarly, rotor voltage Eqs (13, 14) can be derived:

$$v_{rd} = R_r i_{rd} + \frac{d}{dt} \Psi_{rd} - (\omega_s - \omega_m) \Psi_{rq}, \quad (13)$$

$$v_{rq} = R_r i_{rq} + \frac{d}{dt} \Psi_{rq} - (\omega_s - \omega_m) \Psi_{rd}, \quad (14)$$

where stator flux space vector components are Eqs (15–20):

$$\Psi_{sd} = L_s i_{sd} + L_m i_{rd}, \quad (15)$$

$$\Psi_{sq} = L_s i_{sq} + L_m i_{rq}, \quad (16)$$

$$\Psi_{sx} = L_{\sigma s} i_{sx}, \quad (17)$$

$$\Psi_{sy} = L_{\sigma s} i_{sy}, \quad (18)$$

$$\Psi_{s01} = L_{\sigma s} i_{s01}, \quad (19)$$

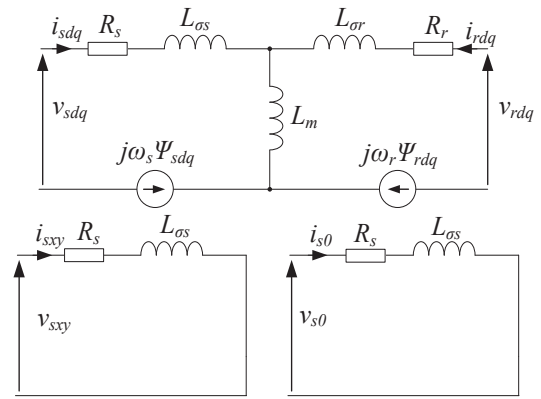


Fig. 3. Scheme of a six-phase stator and three-phase rotor doubly fed induction machine model in a rotating reference frame

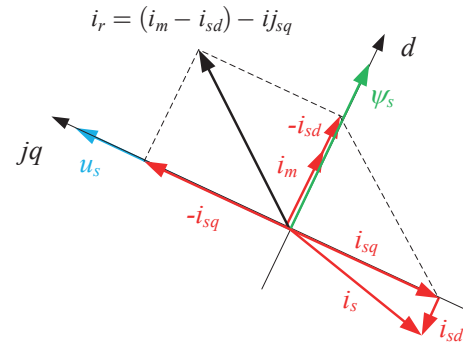


Fig. 4. Vector diagram of a loaded DFIG-DC generator

$$\Psi_{s02} = L_{\sigma s} i_{s02}, \quad (20)$$

and rotor flux space vector components are Eqs (21, 22).

$$\Psi_{rd} = L_r i_{rd} + L_m i_{sd}, \quad (21)$$

$$\Psi_{rq} = L_r i_{rq} + L_m i_{sq}, \quad (22)$$

Currents components on the  $xy$  axis are not induced on the rotor side, due to lack of those components in three-phase systems. Components of the stator current in the  $xy$  and  $0_1 0_2$  reference frames do not produce flux coupled with a rotor and are limited only by resistance and impedance of a stator. For rotor three-phase variables, the  $\alpha\beta$  to  $dq$  transformation is a classic Park's transformation.

Electromagnetic torque can be computed using electromotive force producing components (in the  $dq$  frame):

$$T_e = 3L_m p_b (i_{rd} i_{sq} - i_{sd} i_{rq}), \quad (23)$$

### 3. Control methods of six-phase DFIG-DC

**3.1. Field oriented control of the DFIG-DC generator.** In the described system, the machine rotor is three-phase and thus the  $xy$  and  $0_1 0_2$  components on the rotor side do not exist. Thus,

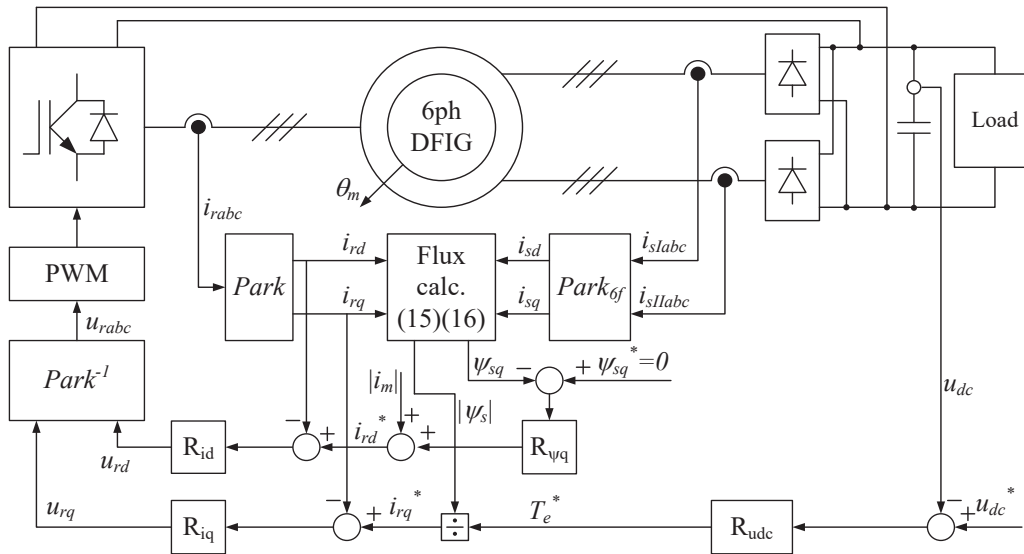


Fig. 5. Scheme of field oriented control for a DFIG-DC system

only  $dq$  current components are used for control of the rotor current space vector. Therefore, the field oriented control FOC method for the six-phase DFIG is similar to the FOC control method for classic DFIG described in [25]. This control system consists of rotor current vector components controllers in the  $dq$  reference frame, as presented in Fig. 5.

The reference  $d$  current vector component is set initially on the magnetizing current level  $i_m$ . The reference  $i_d^*$  component is further adjusted by the flux  $q$  component regulator  $R_{\psi q}$ , which plays the role of a reference frame synchronizer. This ensures orientation of the reference frame along the stator flux vector. The second component of reference rotor current vector  $i_d^*$  is set by the outer controller  $R_{udc}$  responsible for DC bus voltage regulation. Output signal of the  $R_{udc}$  regulator references electromagnetic torque of the machine, which is further scaled

by actual stator flux. Scaling factors such as e.g. the number of pole pairs are taken into consideration in the  $R_{udc}$  controller gain, so they are not shown separately in the scheme.

**3.2. Direct torque control of the DFIG-DC generator.** In literature, the direct torque control (DTC) method is described as effective for reduction of torque pulsations in a three-phase DFIG-DC system [19, 20]. The DTC method for a six-phase DFIG is similar to the DTC control method for a three-phase DFIG, shown in [19]. In multi-phase machines, only  $dq$  components of the current are responsible for production of torque, therefore  $xy$  and  $0_1 0_2$  stator current components are not considered in DTC control. The control system consists of a stator flux module controller and a torque controller, as presented in Fig. 6. The reference flux vector component  $|\psi_{s0}|$  is set at

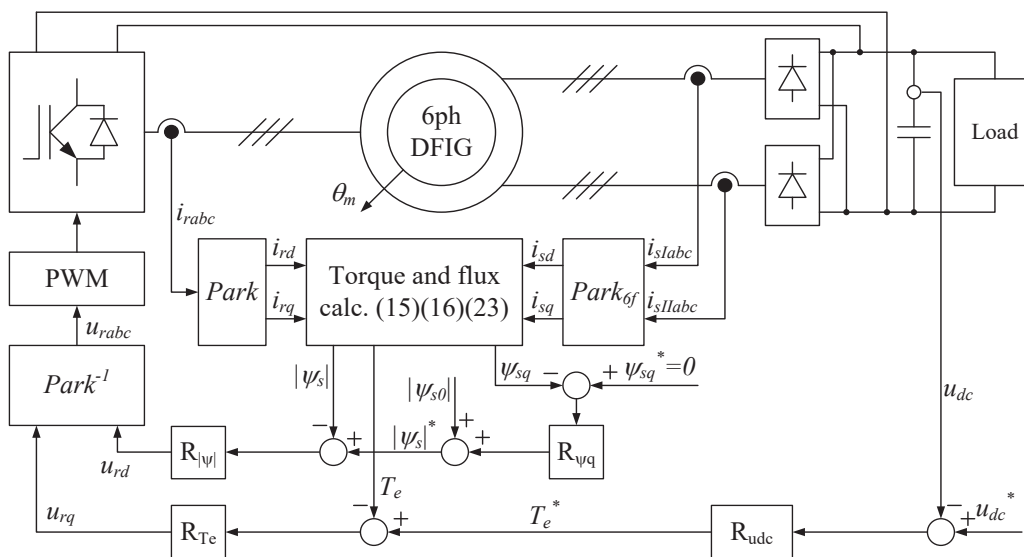


Fig. 6. Scheme of a variant of direct torque control method for a DFIG-DC system

a level giving nominal stator voltage at the frequency of 50 Hz. The reference flux is corrected by an outer  $R_{\psi q}$  controller of the stator flux  $q$  component, playing the role of a reference frame synchronizer. This ensures orientation of the reference frame along the stator flux space vector. Torque is controlled in the parallel control paths and its reference value  $T_e^*$  is set by a DC voltage regulator.

## 4. Simulation results

**4.1. Comparison of three-phase and six-phase machine based DFIG-DC systems with the FOC method.** The proposed six-phase DFIG was modeled in C using Eqs (1–5) and a PSIM simulation environment. Parameters of the modeled DFIG machine are outlined in the Appendix in Table 1. The six-phase asymmetrical DFIG was compared to a three-phase DFIG with the same parameters under the same steady state conditions (fully loaded 2MW DFIG-DC system). Figure 7 presents simulation results of field oriented control of a DFIG-DC system with a three-phase machine.

Significant reduction of both torque pulsations and DC bus voltage oscillations can be observed for the asymmetrical six-phase machine (Fig. 8) in comparison with the three-phase machine (Fig. 7). The frequency of torque and DC bus voltage oscillations is doubled in the six-phase machine as compared with the three-phase machine.

In both cases (for the three-phase machine (Fig. 7) and the six-phase machine (Fig. 8)), adequate position of the reference frame  $d$  axis along the stator flux vector can be observed ( $\psi_{sq} = 0$ ), thanks to the synchronizer applied. In the

Table 1  
Parameters of simulated DFIG DC system

Symbol	Parameter	Value
$P_m$	Rated mechanical power	2 MW
$u_s$	Stator voltage (L-L rms)	690 V
$u_r$	Rotor voltage (L-L rms) (at 0 rpm)	2 kV
$p$	Number of pole pairs	2
$L_m$	Magnetizing inductance	2.5 mH
$L_s$	Stator inductance	2.587 mH
$L_r$	Rotor inductance	2.587 mH
$R_s$	Stator resistance	2.6 m $\Omega$
$R_r$	Rotor resistance	2.6 m $\Omega$
$C_{dc}$	DC bus capacitance	5 mF
$u_{dc}$	DC bus voltage	970 V

six-phase machine based DFIG-DC system, the rotor current contains a smaller amount of harmonics (harmonics related to the 300 Hz frequency component in the  $dq$  frame are naturally eliminated through the use of asymmetrical six-phase stator windings). All tests of 2 pole pairs doubly fed induction machines were made at 1200 rpm, i.e. 80% of synchronous mechanical speed.

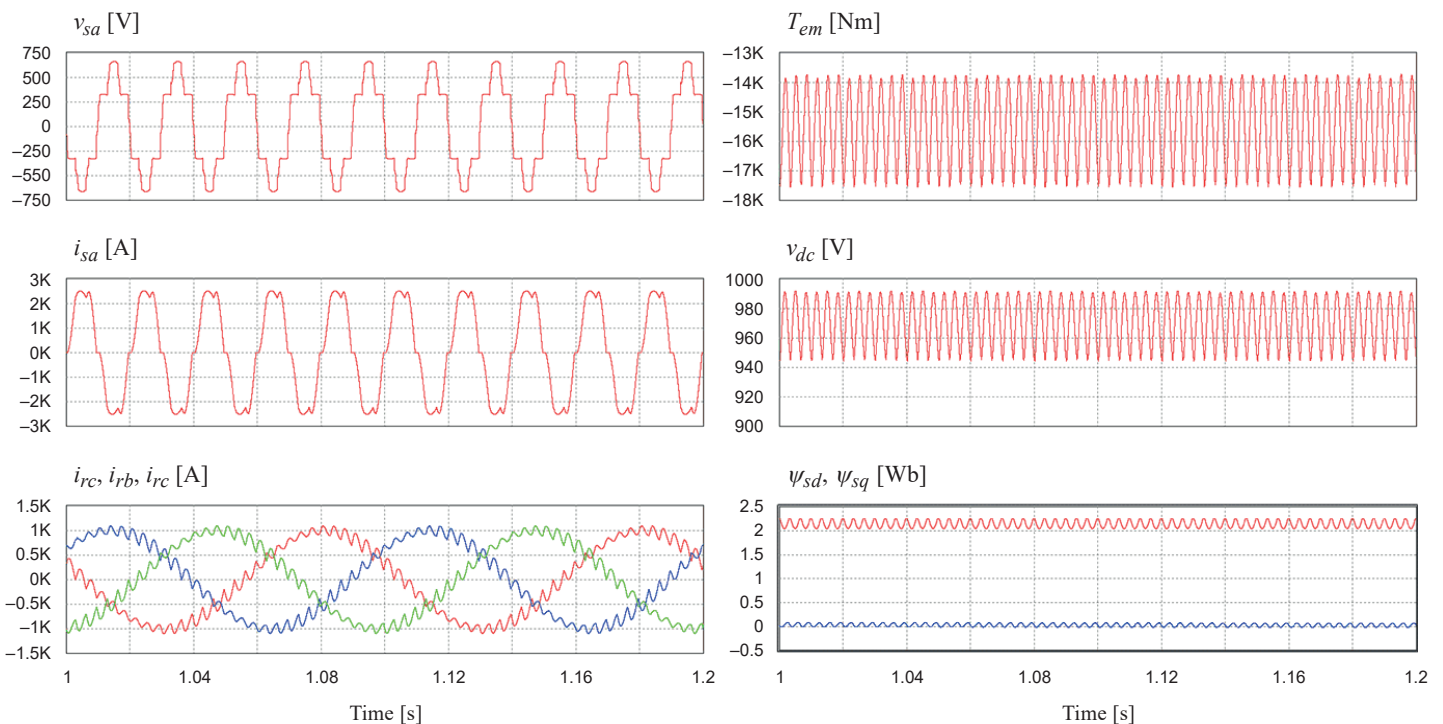


Fig. 7. Simulations results of a 2MW three-phase doubly fed induction machine based standalone DC voltage generator controlled with FOC

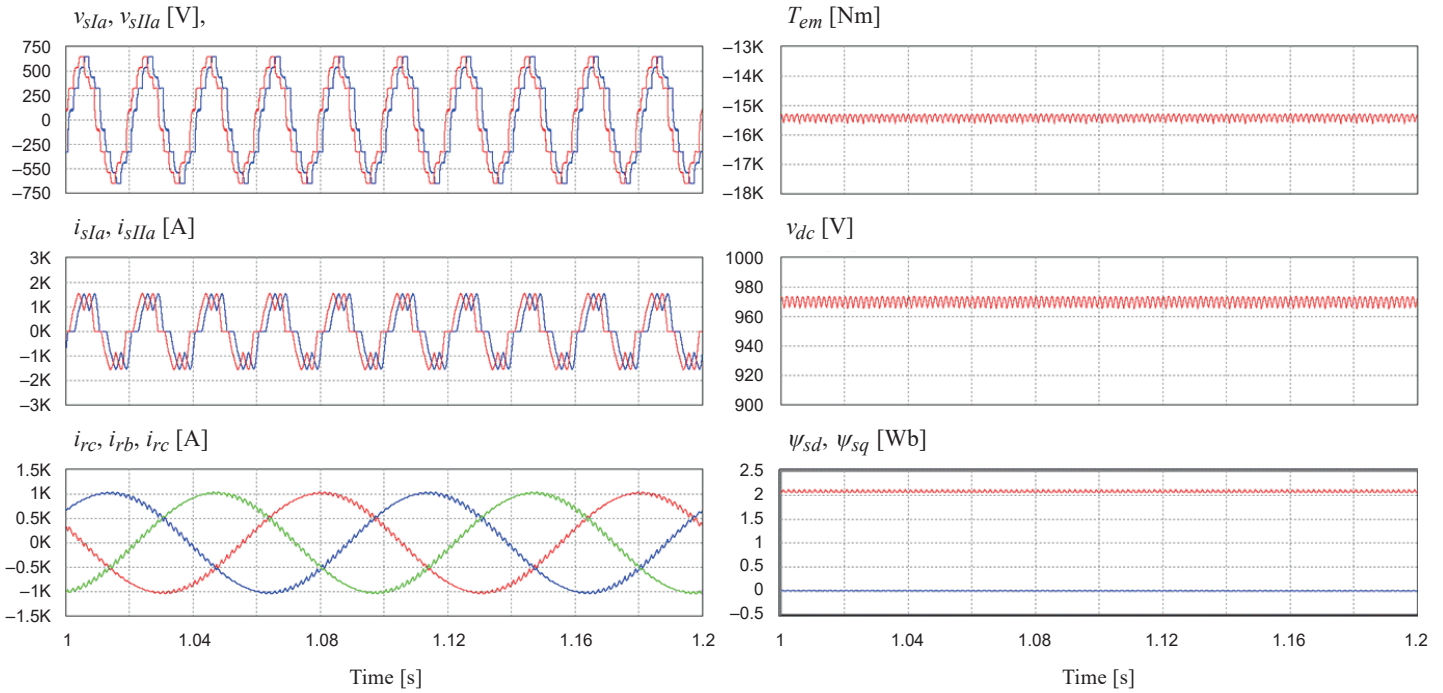


Fig. 8. Simulations results of a 2MW six-phase doubly fed induction machine based standalone DC voltage generator controlled with FOC

**4.2. Comparison of results for a six-phase machine with FOC and DTC control methods.** The direct torque control method was implemented in the simulation environment for the same model of the six-phase machine under the same operating conditions (same DC load resistance and same mechanical speed). Results of simulations for the DTC method are presented in Fig. 9.

Simulation does not prove a significant difference in torque ripple values for both compared methods. DC bus voltage oscillations are visibly lower, but it has to be taken into consideration that this is an ideal simulation. Relative values of DC bus voltage oscillations are in both cases much smaller than in the case of a similar three-phase machine, and we cannot say that in the case of the six-phase machine direct torque control has

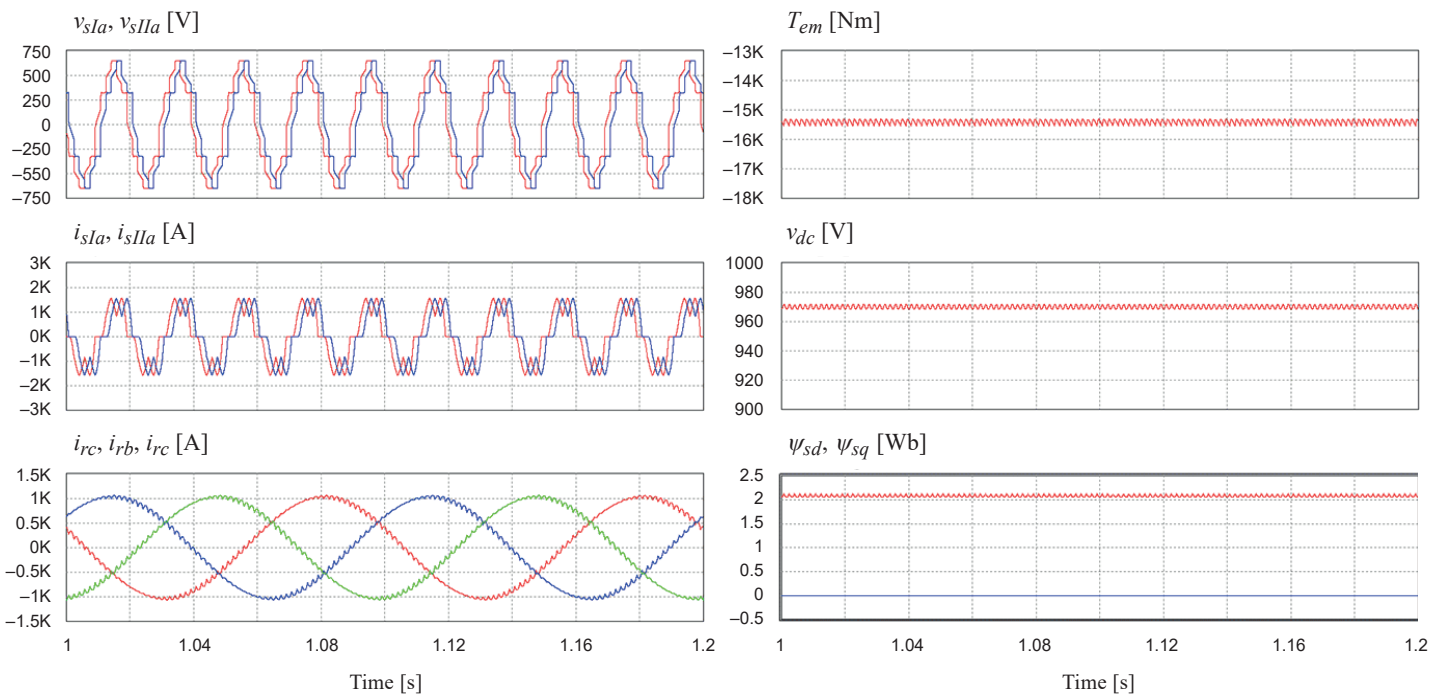


Fig. 9. Simulations results of a 2MW six-phase doubly fed induction machine based standalone DC voltage generator controlled with DTC

Six-phase doubly fed induction machine-based standalone DC voltage generator

significant benefits in comparison with field oriented control methods. On the other hand, field oriented control equipped with current regulators makes it easier to implement over-current protections in the case of DC bus overload, simply by limitation of the current vector length. In the case of direct torque control, no current regulators are used, so current limitation has to be effected outside the main control structure by means of adaptive change of reference torque and flux. This manner of current limitation is not as intuitive as in the FOC method.

**5. Experimental results**

The experimental tests were conducted with a six-phase DFIG connected from the stator side to a twelve-pulse diode rectifier and fed on the three-phase rotor side from a two-level converter connected to a common DC bus (Fig. 10). The generator is driven using a thyristor-converter-fed DC motor drive with speed control. Initial excitation under laboratory conditions is achieved through an additional auxiliary diode rectifier ADR providing initial energy to the common DC bus from the laboratory AC grid.

A view of the power electronic converter and electromechanical system is shown in Fig. 11. The control system of the DFIG-DC system was implemented on a digital signal processing DSP TMS320F28335 microcontroller. Please note that the construction of the induction machine was originally three-phase and eight-pole, and it has been re-wound to a six-phase stator, a three-phase rotor and four poles. Thus, the design is not optimum, and only two stator slots per pole and per phase are obtained, so distortions during machine operation are visible. In industrial practice, it should be designed specifically as a stator six-phase machine.

In subsequent figures, one stator voltage and two stator currents are presented for clarity. Steady state operation

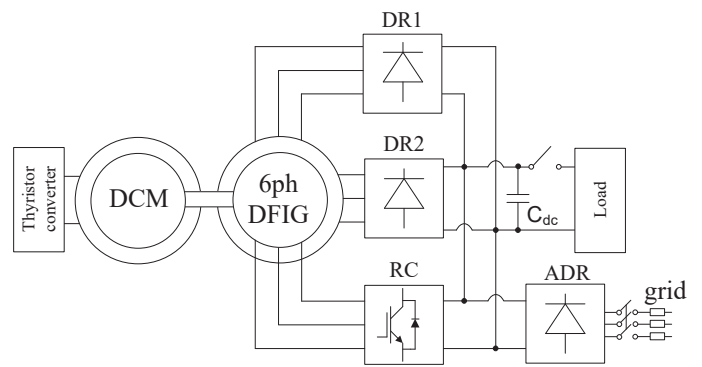


Fig. 10. Scheme of laboratory setup with a six-phase DFIG-DC system

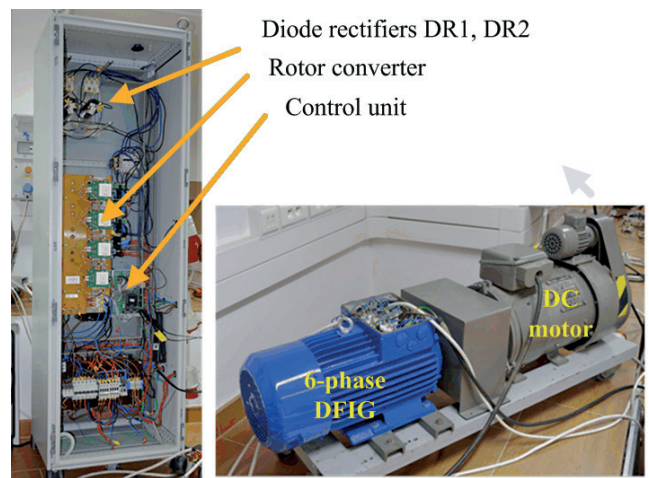


Fig. 11. Laboratory setup with a six-phase DFIG-DC system

of a six-phase DFIG-DC generator is presented in Fig. 12. Step-loading and step-unloading cases are presented in Fig. 13

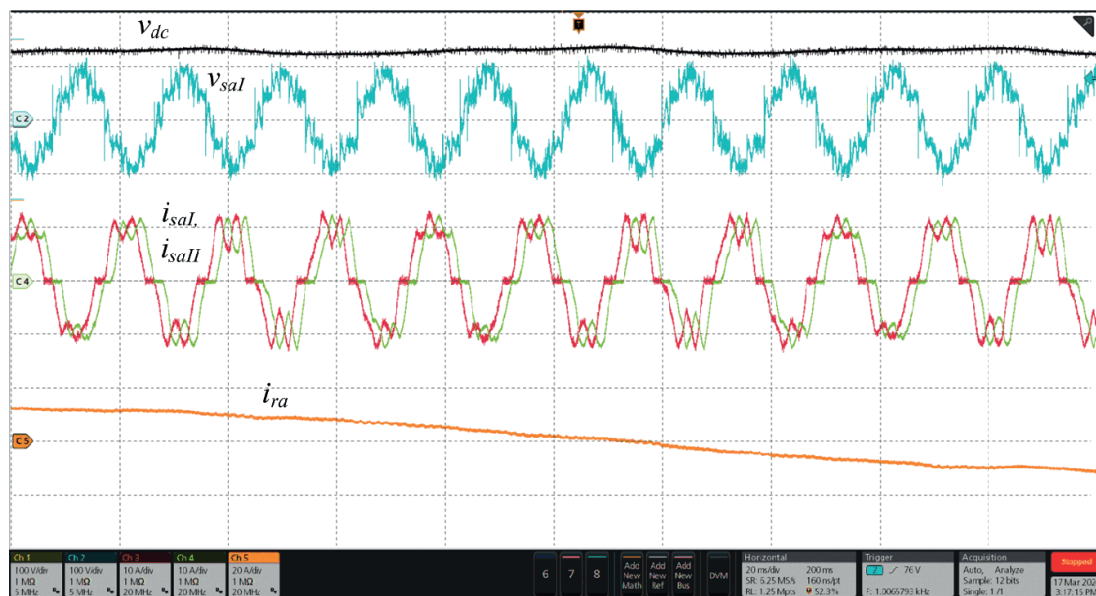


Fig. 12. Experimental results of the six-phase DFIG-DC system controlled by FOC at steady state operation

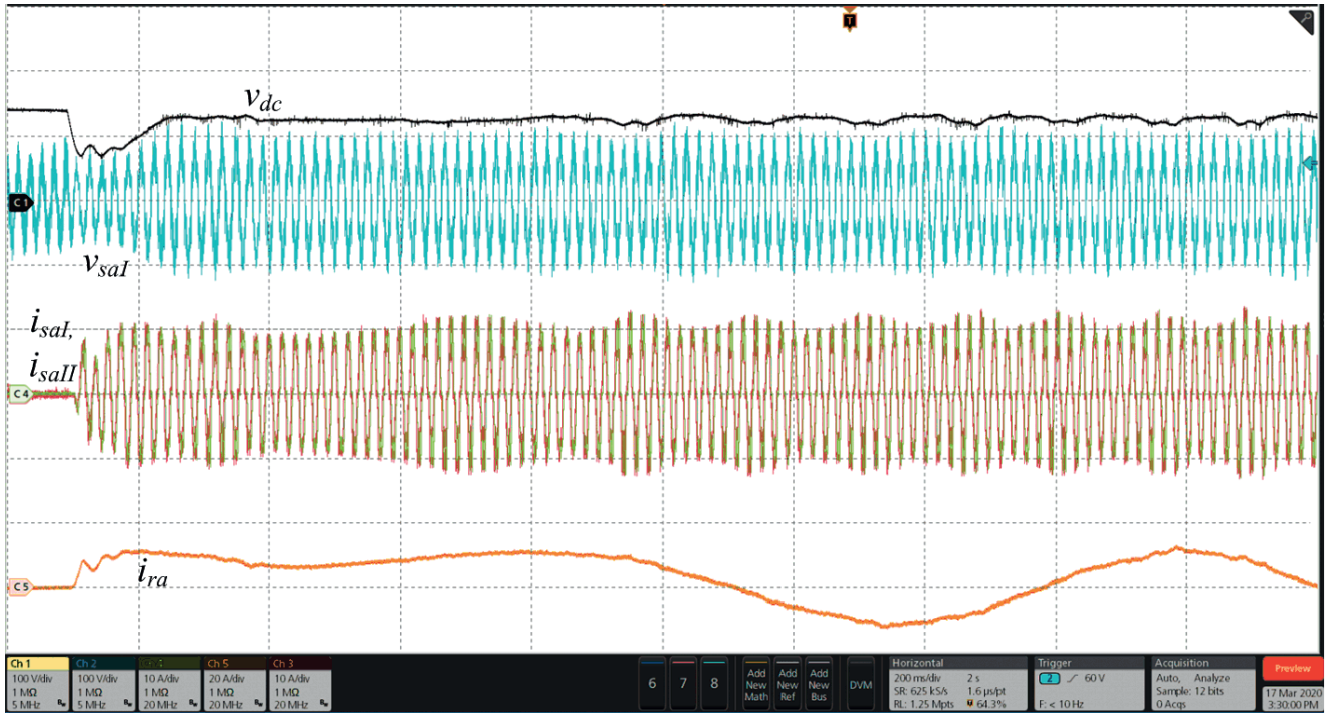


Fig. 13. Experimental results of the six-phase DFIG-DC system controlled by FOC at step-loading

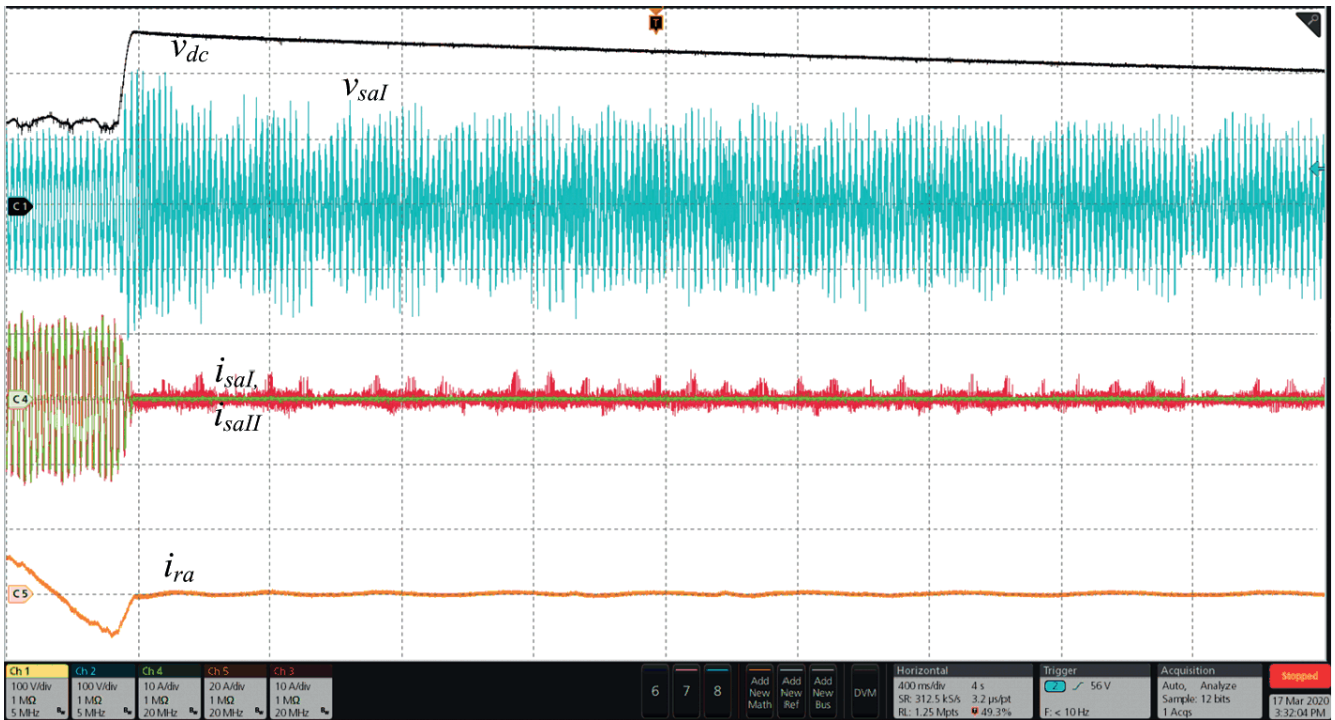


Fig. 14. Experimental results of the six-phase DFIG-DC system controlled by FOC at step-unloading

and Fig. 14, respectively. Variable speed operation results are presented in Fig. 15.

As the magnetic circuit is not designed originally for the six-phase stator wounded induction machine, the results are not fully satisfactory in terms of stator and DC voltage quality.

Regular oscillations depending on rotor position in the stator and rotor currents, as well as in the stator and DC bus voltage, occur. Nevertheless, the system is stable and presents the possibility of DC current regulation using field oriented control. During the step-loading process (Fig. 13), a DC voltage dip

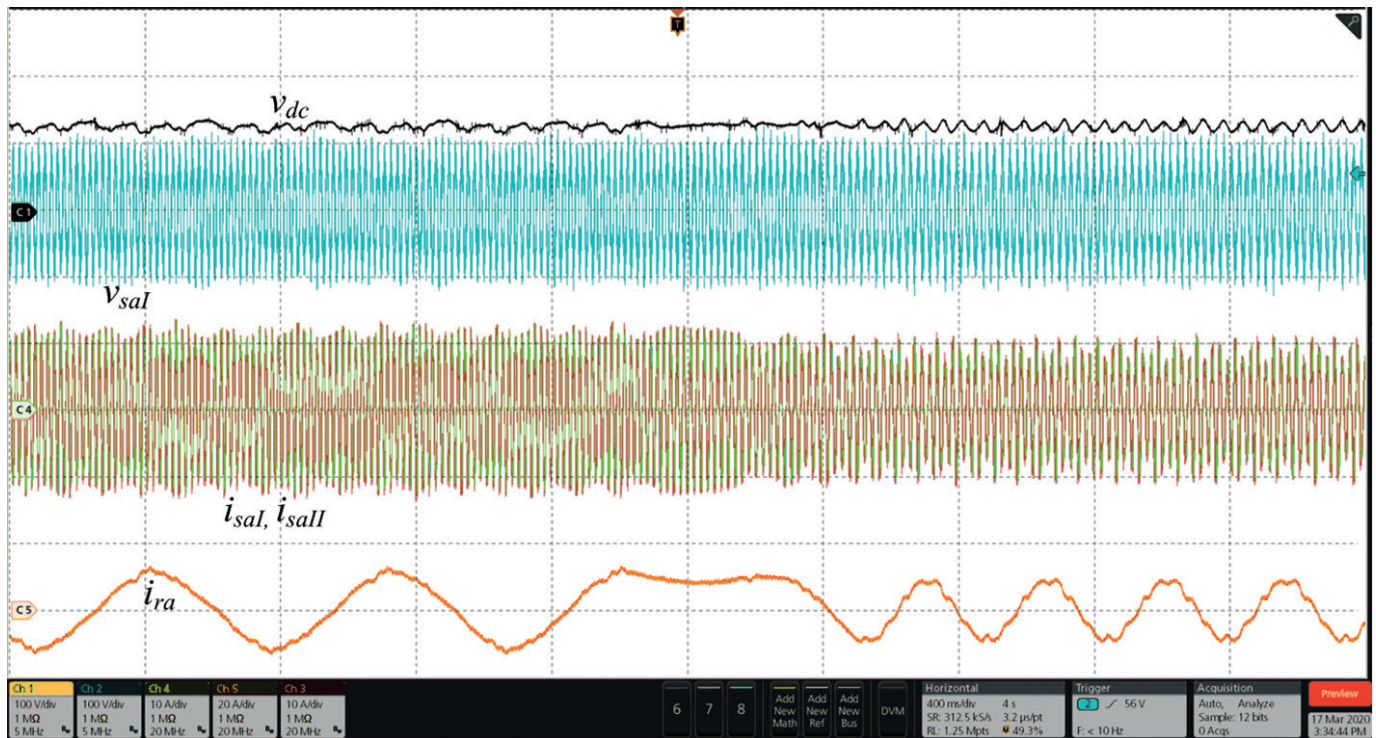


Fig. 15. Experimental results of the six-phase DFIG-DC system controlled by FOC at variable speed operation

occurs during the transient state. The DC bus voltage regulator is relatively fast, but the voltage dip cannot be fully compensated for because of rotor current limitations.

The dynamics of DC voltage regulation can be evaluated in the next figure (Fig. 14), showing step-unloading. The rotor current drops fast, but the energy stored in the machine leakage inductance increases the output DC voltage more than twice. This can be observed not only in the six-phase machine, but also in the three-phase DFIG-DC system. Further voltage decrease is related to energy losses in the rotor power converter and the machine. However, it takes a significantly long time, therefore in a real system, a DC connected breaking chopper is required. It has to be noted that this issue is not described in the literature, whereas some methods proposed in publications prove unstable during no-load operation.

Variable speed operation results registered in Fig. 15 indicate that during super-synchronous speed operation, the rotor and stator currents are smaller than during sub-synchronous speed operation. It confirms that at super-synchronous speed the required torque for the same load power is smaller than during sub-synchronous speed.

## 6. Conclusion

A six-phase stator and three-phase rotor doubly fed induction machine for DC power generation has many advantages. Comparing with classical three-phase construction, significant torque pulsation reduction is achieved naturally, that is only by means of windings configuration without any extra exten-

sions of the control method such as oscillatory terms in current or torque controllers. Reduced power of the rotor side circuit causes the power transferred through existing rotating connection to become insignificant. The three-phase system on the machine rotor side does not increase the number of slip-rings and brushes, so the construction is simpler.

Classic field oriented rotor current control provides good torque oscillations reduction as compared with the direct torque control method. Experimental tests provided in the paper present, albeit to a limited extent, the properties of the six-phase stator DFIG. To fully show the advantages of such a machine, its construction should be designed specifically to avoid the disturbances observed. Nevertheless, the experimental tests show stable operation of the machine controlled by the field oriented rotor current control method under different conditions such as step-loading, step-unloading and variable speed.

## REFERENCES

- [1] G.D. Marques, D. Sousa, and M. F. Iacchetti, "Sensorless torque control of a DFIG connected to a DC link", *IEEE Int. Symp. on Sensorless Control for Electrical Drives and Predictive Control of Electrical Drives and Power Electronics – SLED/PRECEDE'13*, Munich, Germany, 2013, pp. 1–7.
- [2] M.F. Iacchetti and G.D. Marques, "Enhanced torque control in a DFIG connected to a DC grid by a diode rectifier", *16<sup>th</sup> Europ. Conf. Power Electron. and Appl. – EPE'14*, Lappeenranta, Finland, 1–9 (2014).
- [3] G.D. Marques and M.F. Iacchetti, "A self-sensing stator-current-based control system of a DFIG connected to a DC-link", *IEEE Trans. Ind. Electron.* 62(10), 6140–6150 (2015).

- [4] Y. Li, *et al.*, “The capacity optimization for the static excitation controller of the dual-stator-winding induction generator operating in a wide speed range”, *IEEE Trans. Ind. Electron.* 56(2), 530–541 (2009).
- [5] H. Misra, A. Gundavarapu, and A.K. Jain, “Control scheme for DC voltage regulation of stand-alone DFIG-DC system”, *IEEE Trans. Ind. Electron.* 64(4), 2700–2708 (2017).
- [6] N. Yu, H. Nian, and Y. Quan, “A novel DC grid connected DFIG system with active power filter based on predictive current control”, *Int. Conf. Electr. Machines and Systems – ICEMS’11*, Beijing, China, 2011, pp. 1–5.
- [7] M.F. Iacchetti, G.D. Marques, and R. Perini, “Torque ripple reduction in a DFIG-DC system by resonant current controllers”, *IEEE Trans. Power Electron.* 30(8), 4244–4254 (2015).
- [8] C. Wu and H. Nian, “Improved direct resonant control for suppressing torque ripple and reducing harmonic current losses of dfig-dc system”, *IEEE Trans. Power Electron.* 34(9), 8739–8748 (2019).
- [9] C. Wu, *et al.*, “Adaptive repetitive control of DFIG-DC system considering stator frequency variation”, *IEEE Trans. Power Electron.* 34(4), 3302–3312 (2018).
- [10] A. Gundavarapu, H. Misra, and A. K. Jain, “Direct torque control scheme for dc voltage regulation of the standalone DFIG-DC system”, *IEEE Trans. Ind. Electron.* 64(5), 3502–3512 (2017).
- [11] P. Maciejewski and G. Iwanski, “Direct torque control for autonomous doubly fed induction machine based DC generator”, *12<sup>th</sup> Int. Conf. Ecological Vehicles and Renewable Energies – EVER’17*, Monte Carlo, Monaco, 2017, pp. 1–6.
- [12] P. Maciejewski and G. Iwanski, “Study on direct torque control methods of a doubly fed induction machine working as a stand-alone DC voltage generator”, *IEEE Trans. Energy Conv.* (to be published), doi: 10.1109/TEC.2020.3012589.
- [13] M. Gwóźdz *et al.*, “Generator with modulated magnetic flux for wind turbines”, *Bull. Pol. Ac.: Tech.* 65(4), 469–478 (2017).
- [14] E. Levi, *et al.*, “Multiphase induction motor drives – a technology status review”, *IET Electric Power Applications* 1(4), 489–516 (2007).
- [15] F. Bu, Y. Hu, W. Huang, S. Zhuang, and K. Shi, “Wide-speed-range-operation dual stator-winding induction generator DC generating system for wind power applications”, *IEEE Trans. Power Electron.* 30(2), 561–573 (2015).
- [16] B. Zhang *et al.*, “Comparison of 3-, 5-, and 6-phase machines for automotive charging applications”, *IEEE Int. Electric Machines and Drives Conf.* 3, 1357–1362 (2003).
- [17] K.S. Khan, W.M. Arshad, and S. Kanerva, “On performance figures of multiphase machines”, *18<sup>th</sup> Int. Conf. Electr. Machines – ICELMACH’08*, Vilamoura, Portugal, 2008, pp. 1–5.
- [18] S. Williamson and S. Smith, “Pulsating torque and losses in multiphase induction machines”, *IEEE Trans. Ind. Appl.* 39(4), 986–993 (2003).
- [19] P.G. Holmes and N.A. Elsonbaty, “Cycloconverter-excited divided-winding doubly-fed machine as a wind-power convertor”, *IEE Proc. B Electr. Power Appl.* 131(2), 61–69 (1984).
- [20] P. Maciejewski and G. Iwanski, “Modeling of six-phase double fed induction machine for autonomous DC voltage generation”, *10<sup>th</sup> Int. Conf. Ecological Vehicles and Renewable Energies – EVER’15*, Monte Carlo, Monaco, 2015, pp. 1–6.
- [21] G.D. Marques and M.F. Iacchetti, “DFIG topologies for DC networks: a review on control and design features”, *IEEE Trans. Power Electron.* 34(2), 1299–1316 (2019).
- [22] N.K. Mishra, Z. Husain, and M. Rizwan Khan, “DQ reference frames for the simulation of multiphase (six phase) wound rotor induction generator driven by a wind turbine for disperse generation”, *Electr. Power Appl. IET*, 13(11), 1823–1834, (2019).
- [23] R. Bojoi, *et al.*, “Dual-three phase induction machine drives control; A survey”, *IEEJ Trans. Ind. Appl.* 126(4), 420–429 (2006).
- [24] R. Nelson and P. Krause, “Induction machine analysis for arbitrary displacement between multiple winding sets”, *IEEE Trans. Power Appar. Syst.* 93(3), 841–848 (1974).
- [25] D. Forchetti, G. García, and M.I. Valla, “Vector control strategy for a doubly-fed stand-alone induction generator”, *Ind. Electron. Conf. – IECON’12*, Montreal, Canada, 2, 2002, pp. 991–995.

## Appendix

$$\mathbf{R}_s = R_s \begin{bmatrix} 1 & 0 & 0 & 0 & 0 & 0 \\ 0 & 1 & 0 & 0 & 0 & 0 \\ 0 & 0 & 1 & 0 & 0 & 0 \\ 0 & 0 & 0 & 1 & 0 & 0 \\ 0 & 0 & 0 & 0 & 1 & 0 \\ 0 & 0 & 0 & 0 & 0 & 1 \end{bmatrix}, \quad (24)$$

$$\mathbf{R}_r = R_r \begin{bmatrix} 1 & 0 & 0 \\ 0 & 1 & 0 \\ 0 & 0 & 1 \end{bmatrix}, \quad (25)$$

$$\mathbf{L}_r = L_m^s \begin{bmatrix} \frac{L_r^s}{L_m^s} + \cos(0) & \cos\left(\frac{2}{3}\pi\right) & \cos\left(-\frac{2}{3}\pi\right) \\ \cos\left(-\frac{2}{3}\pi\right) & \frac{L_r^s}{L_m^s} + \cos(0) & \cos\left(\frac{2}{3}\pi\right) \\ \cos\left(\frac{2}{3}\pi\right) & \cos\left(-\frac{2}{3}\pi\right) & \frac{L_r^s}{L_m^s} + \cos(0) \end{bmatrix}, \quad (26)$$

## Six-phase doubly fed induction machine-based standalone DC voltage generator

$$\mathbf{L}_s = L_m^s \begin{bmatrix} \frac{L_s^s}{L_m^s} + \cos(0) & \cos(-\alpha) & \cos(-\frac{2}{3}\pi) & \cos(\frac{2}{3}\pi - \alpha) & \cos(-\frac{2}{3}\pi) & \cos(-\frac{2}{3}\pi - \alpha) \\ \cos(-\alpha) & \frac{L_s^s}{L_m^s} + \cos(0) & \cos(-\frac{2}{3}\pi - \alpha) & \cos(\frac{2}{3}\pi) & \cos(-\frac{2}{3}\pi - \alpha) & \cos(-\frac{2}{3}\pi) \\ \cos(\frac{2}{3}\pi) & \cos(-\frac{2}{3}\pi - \alpha) & \frac{L_s^s}{L_m^s} + \cos(0) & \cos(-\alpha) & \cos(\frac{2}{3}\pi) & \cos(\frac{2}{3}\pi - \alpha) \\ \cos(\frac{2}{3}\pi - \alpha) & \cos(-\frac{2}{3}\pi) & \cos(-\alpha) & \frac{L_s^s}{L_m^s} + \cos(0) & \cos(\frac{2}{3}\pi - \alpha) & \cos(\frac{2}{3}\pi) \\ \cos(-\frac{2}{3}\pi) & \cos(\frac{2}{3}\pi) & \cos(\frac{2}{3}\pi) & \cos(-\frac{2}{3}\pi - \alpha) & \frac{L_s^s}{L_m^s} + \cos(0) & \cos(-\alpha) \\ \cos(-\frac{2}{3}\pi - \alpha) & \cos(\frac{2}{3}\pi - \alpha) & \cos(\frac{2}{3}\pi - \alpha) & \cos(-\frac{2}{3}\pi) & \cos(-\alpha) & \frac{L_s^s}{L_m^s} + \cos(0) \end{bmatrix}, \quad (27)$$

$$\mathbf{M}_{rs} = L_m^s \begin{bmatrix} \cos(\theta_r) & \cos(\theta_r - \alpha) & \cos(\theta_r + \frac{2\pi}{3}) & \cos(\theta_r + \frac{2\pi}{3} - \alpha) & \cos(\theta_r + \frac{4\pi}{3}) & \cos(\theta_r + \frac{4\pi}{3} - \alpha) \\ \cos(\theta_r + \frac{4\pi}{3}) & \cos(\theta_r + \frac{4\pi}{3} - \alpha) & \cos(\theta_r) & \cos(\theta_r - \alpha) & \cos(\theta_r + \frac{2\pi}{3}) & \cos(\theta_r + \frac{2\pi}{3} - \alpha) \\ \cos(\theta_r + \frac{2\pi}{3}) & \cos(\theta_r + \frac{2\pi}{3} - \alpha) & \cos(\theta_r + \frac{4\pi}{3}) & \cos(\theta_r + \frac{4\pi}{3} - \alpha) & \cos(\theta_r) & \cos(\theta_r - \alpha) \end{bmatrix}, \quad (28)$$

$$\mathbf{M}_{sr} = L_m^s \begin{bmatrix} \cos(\theta_r) & \cos(\theta_r + \frac{2\pi}{3}) & \cos(\theta_r + \frac{4\pi}{3}) \\ \cos(\theta_r + \alpha) & \cos(\theta_r + \frac{2\pi}{3} + \alpha) & \cos(\theta_r + \frac{4\pi}{3} + \alpha) \\ \cos(\theta_r + \frac{4\pi}{3}) & \cos(\theta_r) & \cos(\theta_r + \frac{2\pi}{3}) \\ \cos(\theta_r + \frac{4\pi}{3} + \alpha) & \cos(\theta_r + \alpha) & \cos(\theta_r + \frac{2\pi}{3} + \alpha) \\ \cos(\theta_r + \frac{2\pi}{3}) & \cos(\theta_r + \frac{4\pi}{3}) & \cos(\theta_r) \\ \cos(\theta_r + \frac{2\pi}{3} + \alpha) & \cos(\theta_r + \frac{4\pi}{3} + \alpha) & \cos(\theta_r + \alpha) \end{bmatrix}, \quad (29)$$

$$\frac{d}{d\theta} \mathbf{M}_{sr} = L_m^s \begin{bmatrix} -\sin(\theta_r) & -\sin(\theta_r + \frac{2\pi}{3}) & -\sin(\theta_r + \frac{4\pi}{3}) \\ -\sin(\theta_r + \alpha) & -\sin(\theta_r + \frac{2\pi}{3} + \alpha) & -\sin(\theta_r + \frac{4\pi}{3} + \alpha) \\ -\sin(\theta_r + \frac{4\pi}{3}) & -\sin(\theta_r) & -\sin(\theta_r + \frac{2\pi}{3}) \\ -\sin(\theta_r + \frac{4\pi}{3} + \alpha) & -\sin(\theta_r + \alpha) & -\sin(\theta_r + \frac{2\pi}{3} + \alpha) \\ -\sin(\theta_r + \frac{2\pi}{3}) & -\sin(\theta_r + \frac{4\pi}{3}) & -\sin(\theta_r) \\ -\sin(\theta_r + \frac{2\pi}{3} + \alpha) & -\sin(\theta_r + \frac{4\pi}{3} + \alpha) & -\sin(\theta_r + \alpha) \end{bmatrix}, \quad (30)$$

$$\mathbf{T}_{6f} = \frac{1}{3} \begin{bmatrix} \cos(\theta) & \cos(\theta + \alpha) & \cos(\theta + \frac{2}{3}\pi) & \cos(\theta + \frac{2}{3}\pi + \alpha) & \cos(\theta - \frac{2}{3}\pi) & \cos(\theta - \frac{2}{3}\pi + \alpha) \\ -\sin(\theta) & -\sin(\theta + \alpha) & -\sin(\theta + \frac{2}{3}\pi) & -\sin(\theta + \frac{2}{3}\pi + \alpha) & -\sin(\theta - \frac{2}{3}\pi) & -\sin(\theta - \frac{2}{3}\pi + \alpha) \\ \cos(\theta) & -\cos(\theta + \alpha) & \cos(\theta - \frac{2}{3}\pi) & -\cos(\theta - \frac{2}{3}\pi + \alpha) & \cos(\theta + \frac{2}{3}\pi) & -\cos(\theta + \frac{2}{3}\pi + \alpha) \\ -\sin(\theta) & \sin(\theta + \alpha) & -\sin(\theta - \frac{2}{3}\pi) & \cos(\theta - \frac{2}{3}\pi + \alpha) & -\sin(\theta + \frac{2}{3}\pi) & \sin(\theta + \frac{2}{3}\pi + \alpha) \\ 1 & 0 & 1 & 0 & 1 & 0 \\ 0 & 1 & 0 & 1 & 0 & 1 \end{bmatrix}, \quad (31)$$

$$\mathbf{T}_{6f}^{-1} = \frac{1}{3} \begin{bmatrix} \cos(\theta) & -\sin(\theta) & \cos(\theta) & -\sin(\theta) & 1 & 0 \\ \cos(\theta + \alpha) & -\sin(\theta + \alpha) & -\cos(\theta + \alpha) & \sin(\theta + \alpha) & 0 & 1 \\ \cos(\theta + \frac{2}{3}\pi) & -\sin(\theta + \frac{2}{3}\pi) & \cos(\theta + \frac{2}{3}\pi) & -\sin(\theta + \frac{2}{3}\pi) & 1 & 0 \\ \cos(\theta + \frac{2}{3}\pi + \alpha) & -\sin(\theta + \frac{2}{3}\pi + \alpha) & -\cos(\theta + \frac{2}{3}\pi + \alpha) & \sin(\theta + \frac{2}{3}\pi + \alpha) & 0 & 1 \\ \cos(\theta - \frac{2}{3}\pi) & -\sin(\theta - \frac{2}{3}\pi) & \cos(\theta - \frac{2}{3}\pi) & -\sin(\theta - \frac{2}{3}\pi) & 1 & 0 \\ \cos(\theta - \frac{2}{3}\pi + \alpha) & -\sin(\theta - \frac{2}{3}\pi + \alpha) & -\cos(\theta - \frac{2}{3}\pi + \alpha) & \sin(\theta - \frac{2}{3}\pi + \alpha) & 0 & 1 \end{bmatrix}, \quad (32)$$